

X-ray

Generation, properties, applications

The mysterious X-ray



Wilhelm Konrad
Röntgen
(1845-1923)
Nobel prize, 1901

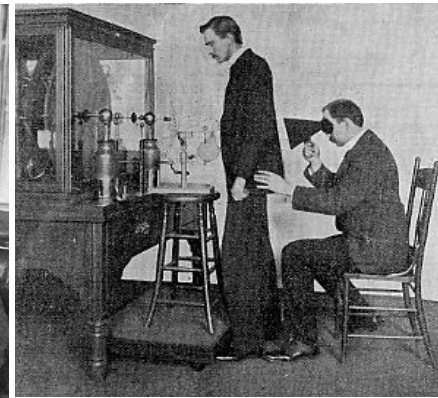
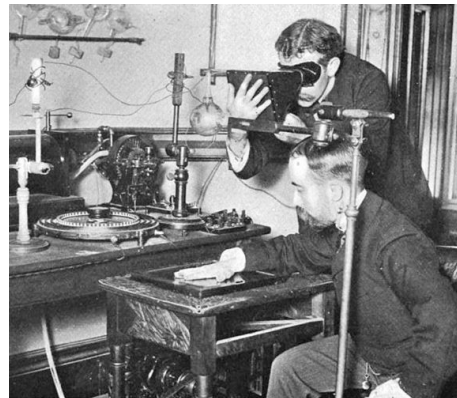
Sitzungs-Berichte der Physikalisch-medicinischen Gesellschaft zu WÜRZBURG.		
Jahrgang 1895.	Der Abonnementspreis pro Jahrgang beträgt M. 4.—. Die Nummern werden einzeln nicht abgegeben. Grössere Beiträge erscheinen in Sonderdrucken.	No. 9.
Verlag der Stahel'schen K. Hof- und Universitäts-Buch- und Kunsthandlung in Würzburg.		
<p>Inhalt. <i>Konrad Rieger</i>: Demonstration des sogenannten „Vogelkopfkablen“ <i>Dóboš Janos aus Battonya in Ungarn</i> (Fortsetzung), pag. 129. — <i>W. C. Röntgen</i>: Ueber eine neue Art von Strahlen, pag. 132. — <i>Wilhelm Wislicenus</i>: 46. Jahresbericht der physikalisch-medicinischen Gesellschaft zu Würzburg, pag. 142. — Mitglieder-Verzeichniss, pag. 146.</p>		
<p>Am 28. Dezember wurde als Beitrag eingereicht: W. C. Röntgen: Ueber eine neue Art von Strahlen. (Vorläufige Mittheilung.)</p>		
<p>1. Lässt man durch eine <i>Hittorfsche</i> Vacuumröhre, oder einen genügend evacuirten <i>Lenard'schen</i>, <i>Crookes'schen</i> oder ähnlichen Apparat die Entladungen eines grösseren <i>Ruhmkorff's</i> gehen und bedeckt die Röhre mit einem ziemlich eng anliegenden Mantel aus dünnem, schwarzem Carton, so sieht man in dem vollständig verdunkelten Zimmer einen in die Nähe des Apparates gebrachten, mit <i>Bariumplatincyannür</i> angestrichenen Papierschirm bei jeder Entladung hell aufleuchten, fluoresciren, gleichgültig ob die angestrichene oder die andere Seite des Schirmes dem Entladungsapparat zugewendet ist. Die Fluorescenz ist noch in 2 m Entfernung vom Apparat bemerkbar.</p>		
<p>Man überzeugt sich leicht, dass die Ursache der Fluorescenz vom Entladungsapparat und von keiner anderen Stelle der Leitung ausgeht.</p>		
<p>2. Das an dieser Erscheinung zunächst Auffallende ist, dass durch die schwarze Cartonhülle, welche keine sichtbaren oder ultravioletten Strahlen des Sonnen- oder des elektrischen Bogenlichtes durchlässt, ein Agens hindurchgeht, das im Stande ist, lebhaft Fluorescenz zu erzeugen, und man wird deshalb wohl zuerst untersuchen, ob auch andere Körper diese Eigenschaft besitzen.</p>		
<p>Man findet bald, dass alle Körper für dasselbe durchlässig sind, aber in sehr verschiedenem Grade. Einige Beispiele führe ich an. Papier ist sehr durchlässig: ¹⁾ hinter einem eingebun-</p>		
<p>¹⁾ Mit „Durchlässigkeit“ eines Körpers bezeichne ich das Verhältniss der Helligkeit eines dicht hinter dem Körper gehaltenen Fluorescenzschirmes zu derjenigen Helligkeit des Schirmes, welcher dieser unter denselben Verhältnissen aber ohne Zwischenschaltung des Körpers zeigt.</p>		



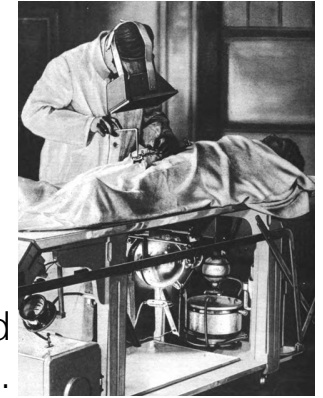
Hand mit Ringen (Hand with Ring): Wilhelm Röntgen's first "medical" X-ray, of his wife's, Anna Bertha Ludwig's hand, taken on 22 December 1895 and presented to Professor Ludwig Zehnder of the Physik Institut (University of Freiburg, 1 January 1896).

Glorious history of x-ray

Transparency –
paper funnel
radioscope



Late
1890s



World
war I.

Everyday
applications



Shoe-fitting
fluoroscope
(1930-50)

CERTIFICATE

SHOE-FITTING TEST DATA FOR _____

1. ANKLE ROLL GOOD ☐ FAIR ☐ POOR ☐

2. WEIGHT DISTRIBUTION

3. X-RAY FITTING TEST

LEFT RIGHT LEFT RIGHT

% BALL % % BALL %

% OUTER % % OUTER %

% HEEL % % HEEL %

RIGHT WAY WRONG WAY RIGHT WAY WRONG WAY

GOOD FAIR POOR GOOD FAIR POOR

RIGHT WAY WRONG WAY RIGHT WAY WRONG WAY

This scientific way of approaching the problem of poorly-fitted shoes eliminates guesswork. Now you can see for yourself!

Airport
security



Medical
applications



1940



1950

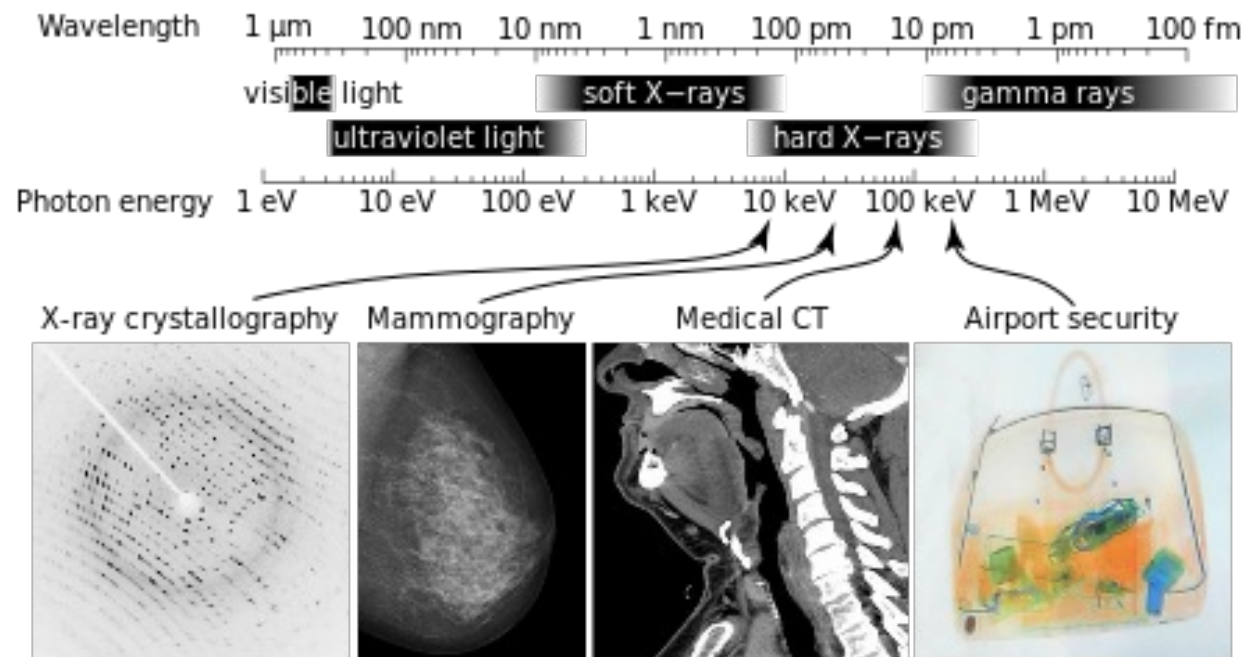


Today



Photon-counting CT

X-rays are electromagnetic waves



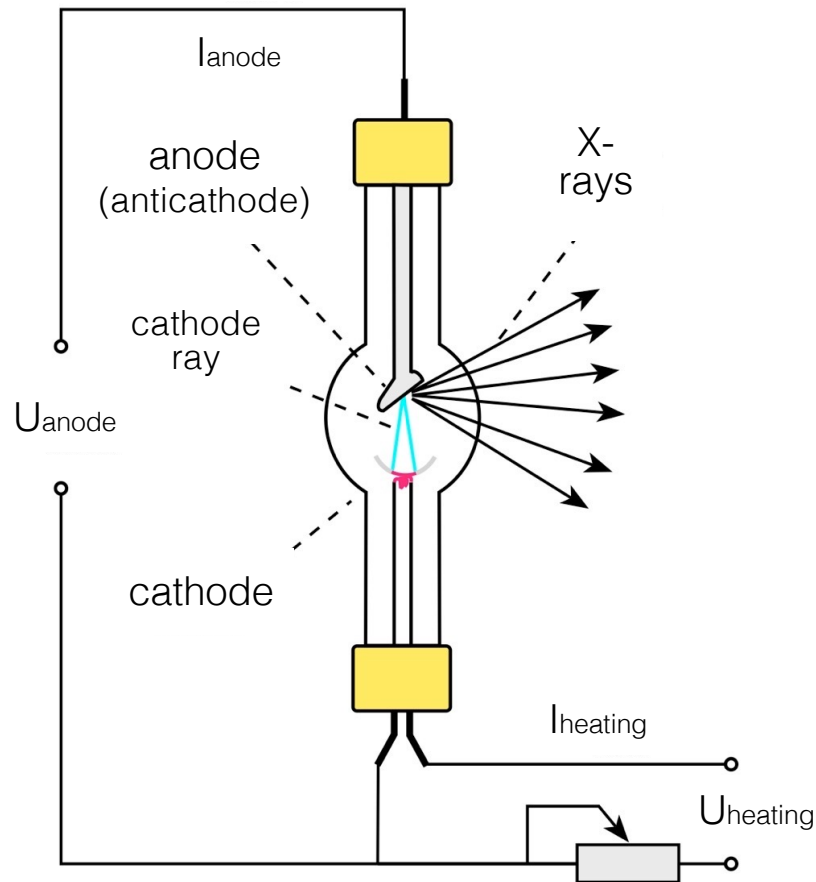
Wavelength 10 - 0.01 nm.

Frequency 30×10^{15} - 30×10^{18} Hz (petahertz - exahertz).

Energy above 100 eV, diagnostic: 20 keV - 200 keV

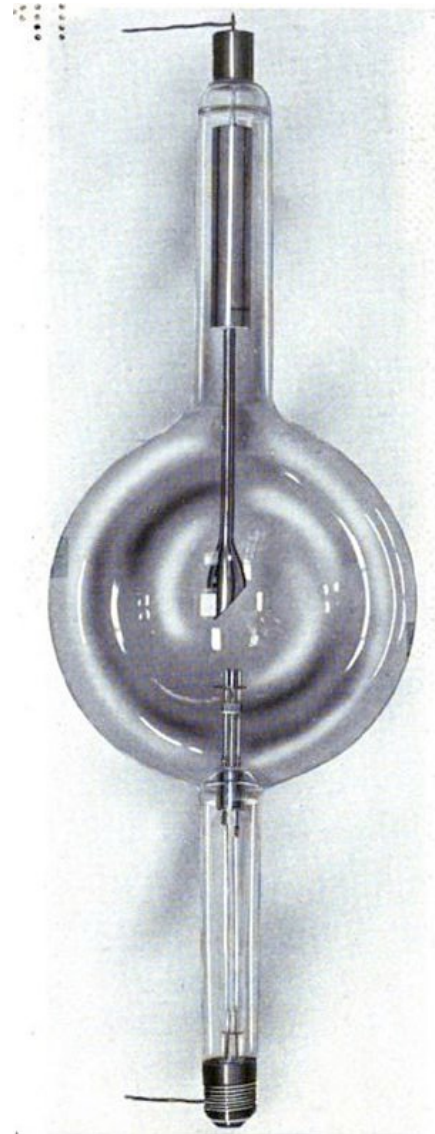
Generation of X-ray

X-ray tube



Steps of X-ray generation:

1. Thermal emission of electrons from cathode
2. Acceleration of free electrons in vacuum
3. Deceleration of free electrons in the target anode



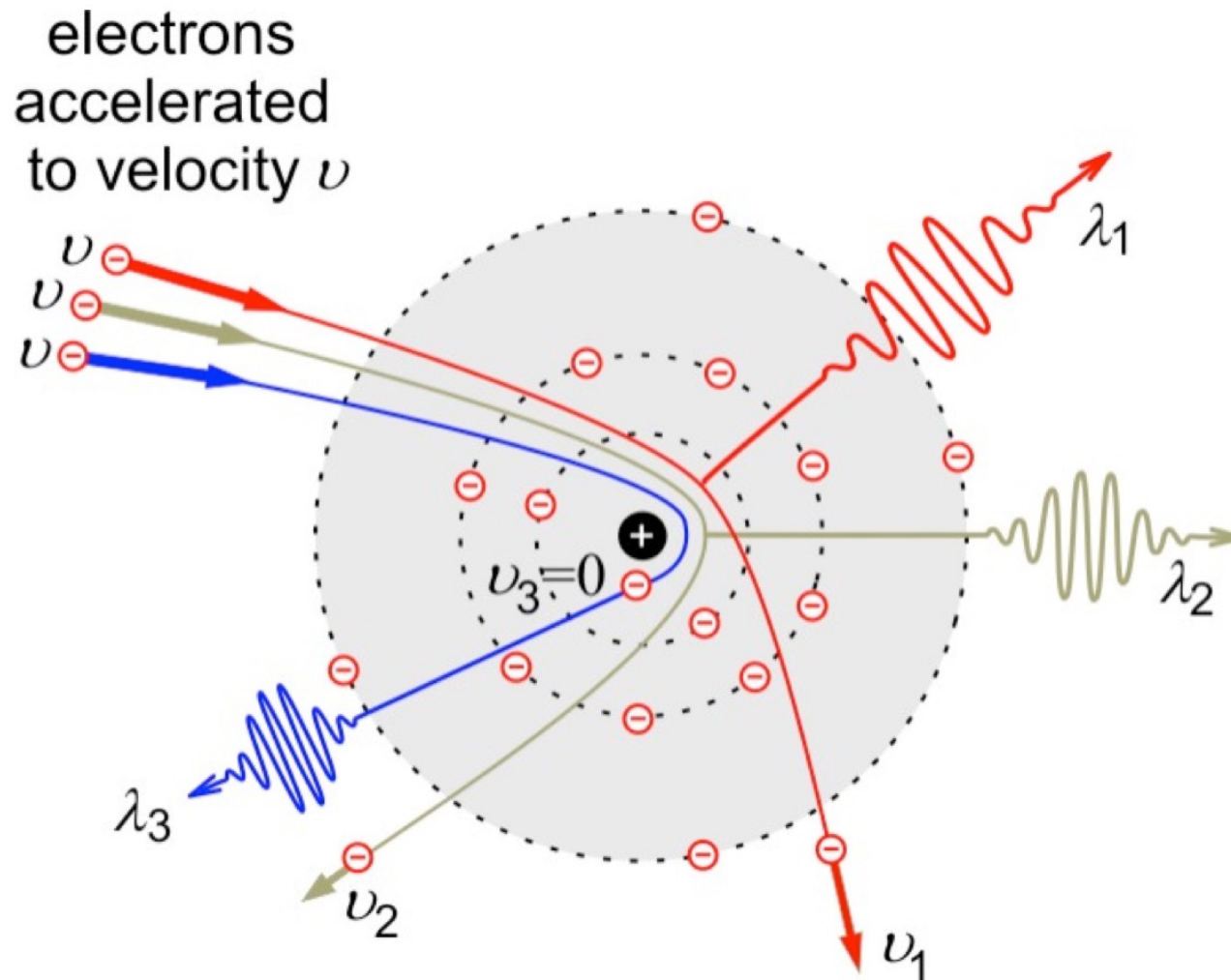
Coolidge x-ray tube (1900s). Heated cathode on the left, anode target on the right. x-ray emitted downwards.



Rotating-anode X-ray tube. Anode rotation is used for cooling.

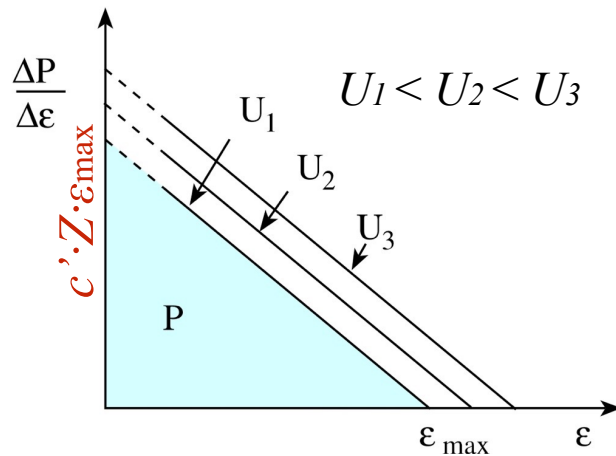
Mechanism I. “Bremsstrahlung”

Electrons *decelerate*, thereby loose their kinetic energy, when interacting with the atoms of the anode (“braking radiation”).



Spectrum of Bremsstrahlung

Continuous



$$eU_{anode} = \varepsilon_{\max} = hf_{\max}$$

Maximal photon energy (ε_{\max})

N.B.: Total kinetic energy of electron is transformed in one step (rare event).

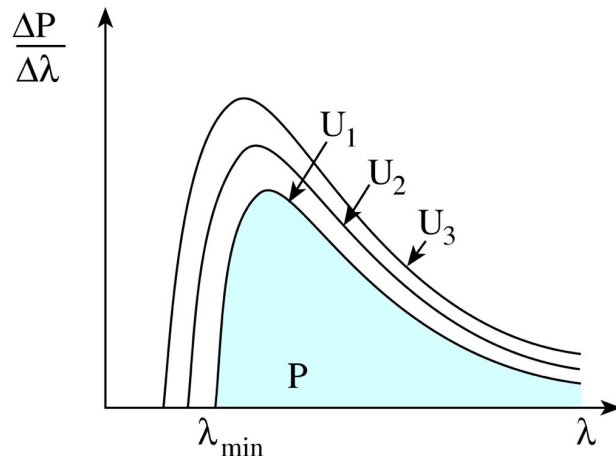
e : electron's charge;
 U_{anode} : accelerating voltage;
 eU_{anode} : acceleration work;
 h : Planck's constant;
 f_{\max} : limiting frequency

$$\lambda_{\min} = \frac{hc}{e} \cdot \frac{1}{U_{anode}}$$

Limiting wavelength (λ_{\min})
 (Duane-Hunt Law)

N.B.: Limiting wavelength is inversely proportional to accelerating voltage.

c : light speed;
 hc/e : constant (1239.8 kV·pm)



$$\frac{\Delta P}{\Delta \varepsilon} = c \cdot Z \cdot (\varepsilon_{\max} - \varepsilon)$$

Energy spectrum
 (energy dependence of power)

$$P_{\text{tot}} = \frac{1}{2} c \cdot Z \cdot \varepsilon_{\max}^2 = c \cdot Z \cdot U_{anode}^2 \cdot e^2$$

$$P_{\text{tot}} = C_{Rtg} \cdot I_{anode} \cdot U_{anode}^2 \cdot Z$$

Total power (P_{tot})

(based on the area of the triangle)

C_{Rtg} : coefficient ($1.1 \times 10^{-9} \text{ V}^{-1}$);
 I_{anode} : anode current (number of electrons hitting the anode per unit time);
 Z : atomic number of the anode atoms

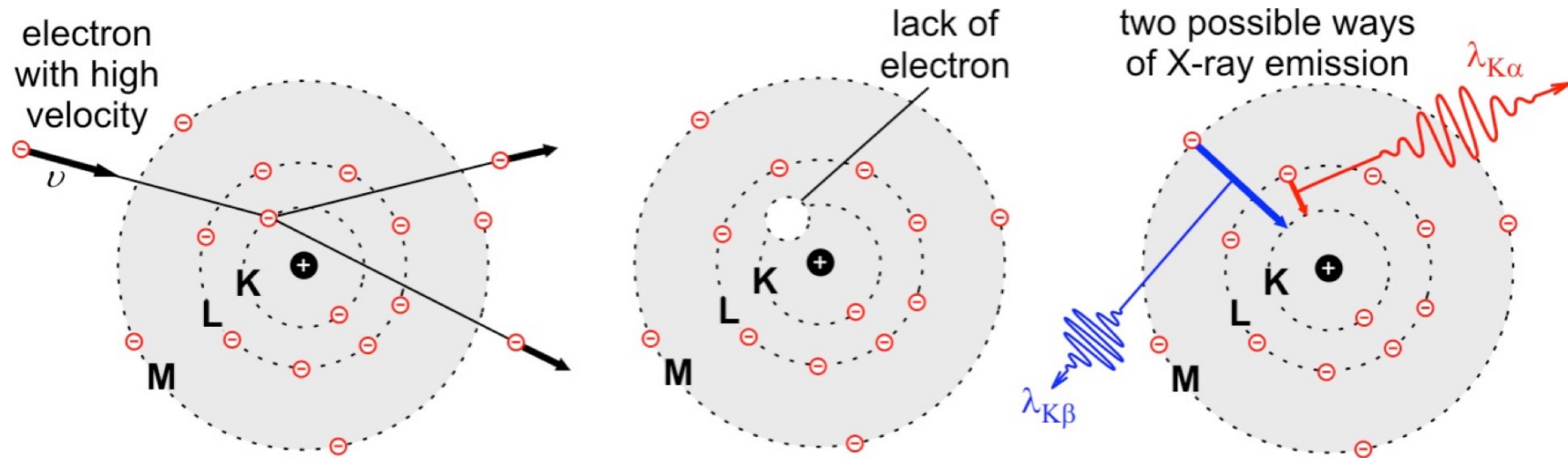
$$\eta = \frac{P_{\text{tot}}}{P_{\text{in}}} = \frac{C_{Rtg} \cdot I_{anode} \cdot U_{anode}^2 \cdot Z}{I_{anode} \cdot U_{anode}} = C_{Rtg} \cdot U_{anode} \cdot Z$$

Efficiency (η)

P_{in} : invested power
 N.B.: Typically, $\eta < 1\%$.

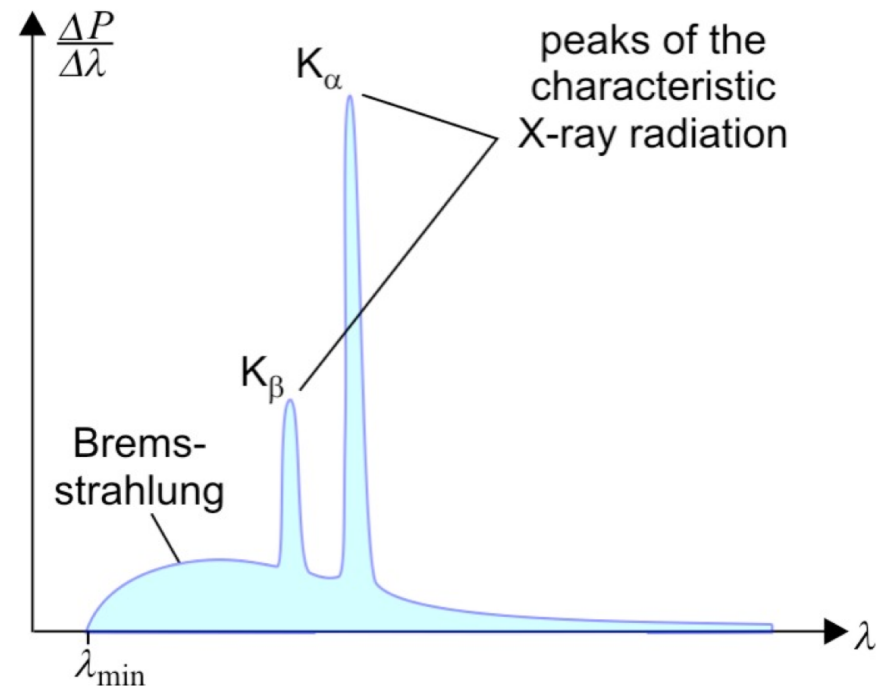
Mechanism II. Characteristic X-ray

Knocked-out inner-shell electron is replaced by one on a higher-energy shell



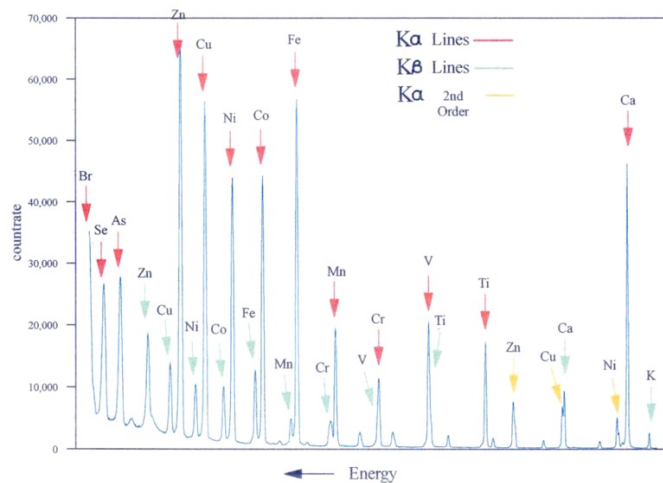
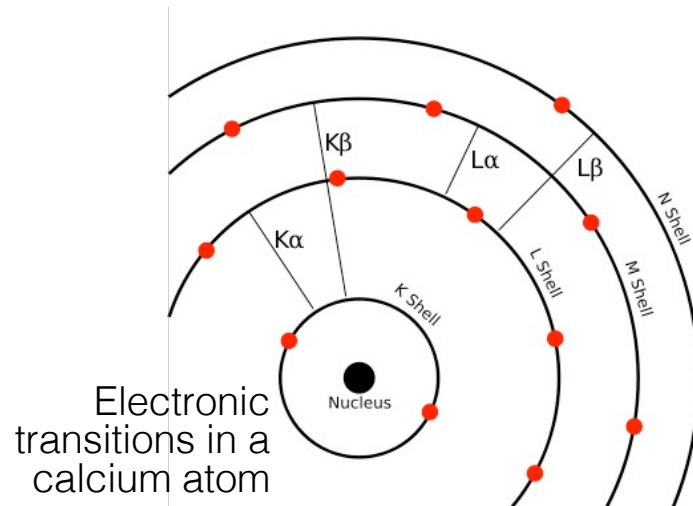
Spectrum of
characteristic X-ray

Line

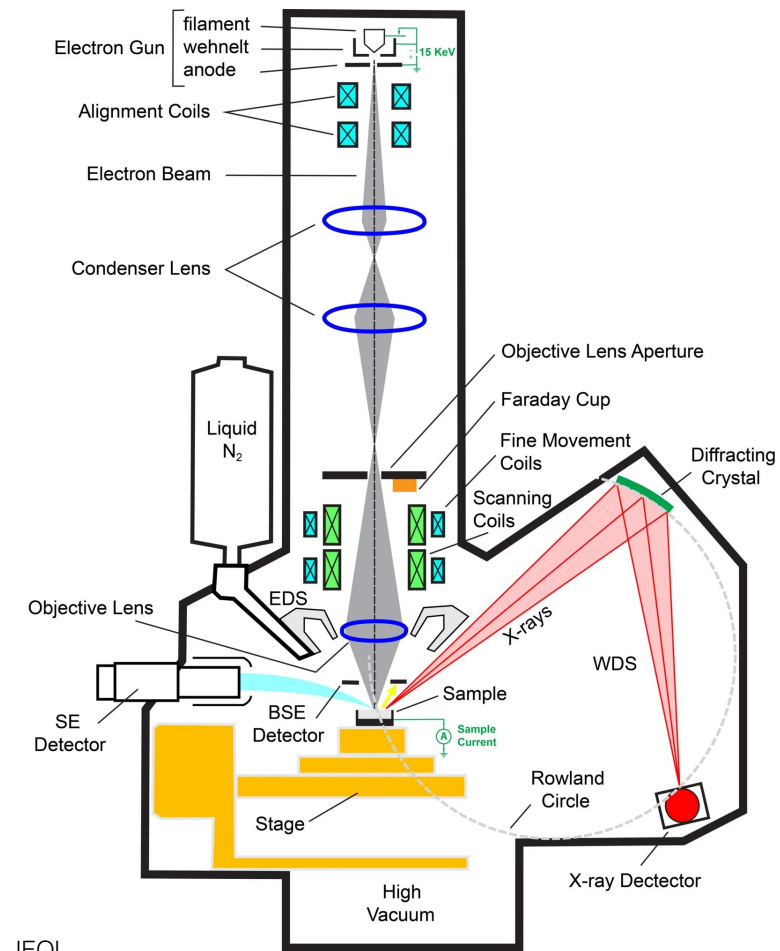


X-ray spectrum characterizes *atomic* composition

Because inner-shell electrons participate in characteristic X-radiation, only the *atomic* (and not the molecular) properties are revealed



Energy dispersive X-ray fluorescence spectrum

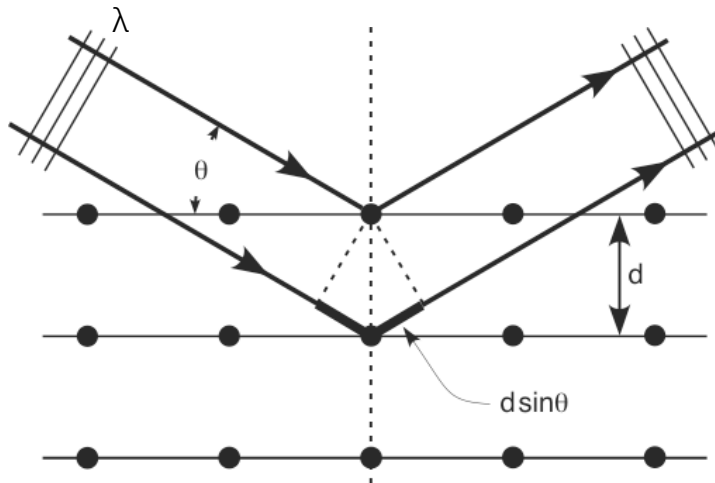


JEOL

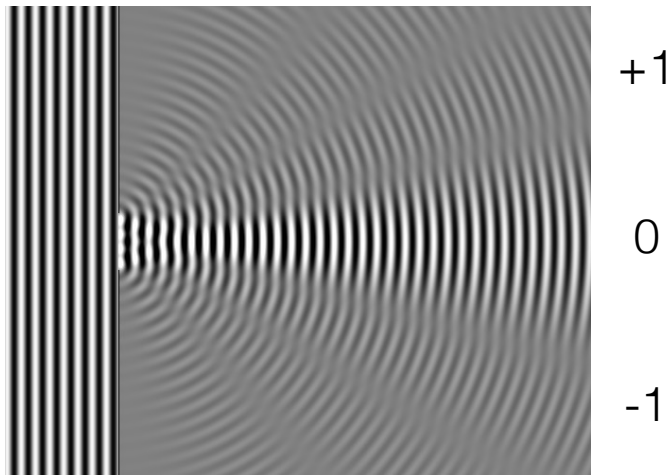
X-ray spectroscope (in an electron microscope!)
(measures x-ray energy spectrum)

Interaction of x-ray with matter

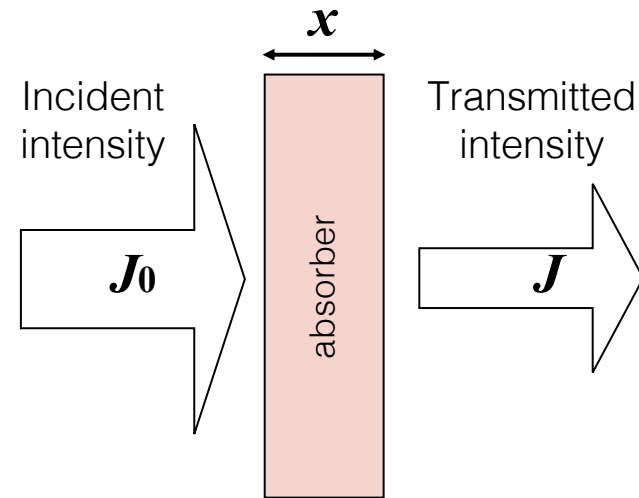
1. Diffraction



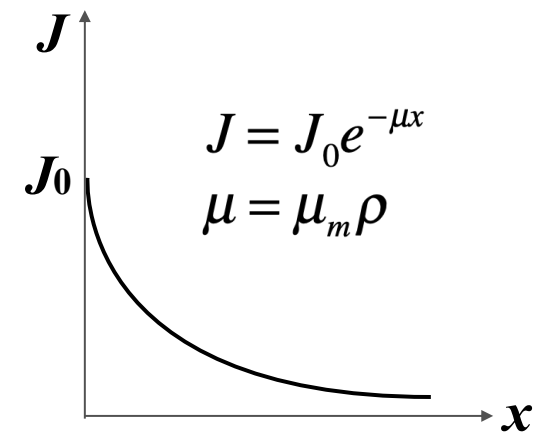
Condition of constructive interference: $2d \sin \theta = n\lambda$



2. Absorption

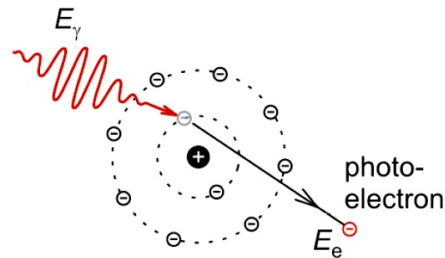


Exponential attenuation principle



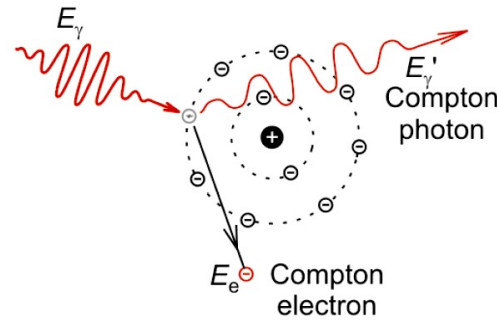
μ : linear attenuation coefficient
 μ_m : mass attenuation coefficient (cm^2/g)
 ρ : density (g/cm^3)

Attenuation mechanisms



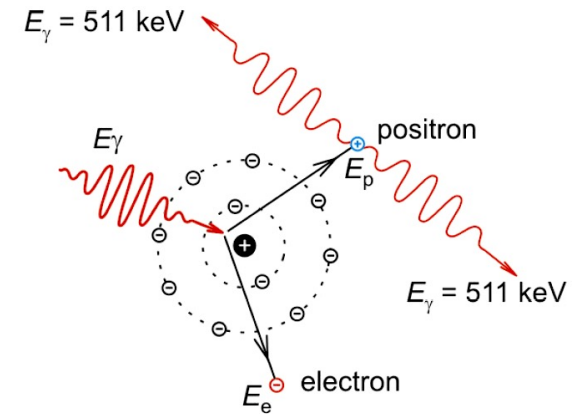
a.) **photoeffect**
 $E_\gamma = A + E_e$
 A = work function
 (escape energy)

$$\tau = \tau_m \rho$$



b.) **Compton scattering**
 $E_\gamma = A + E_e + E'_\gamma$

$$\sigma = \sigma_m \rho$$



c.) **pair production, annihilation**
 $E_\gamma = 2 m_e c^2 + E_e + E_p$
 (if $E_\gamma > 1022 \text{ keV}$)

$$\kappa = \kappa_m \rho$$

τ_m , σ_m , κ_m : mass attenuation coefficients, ρ : density

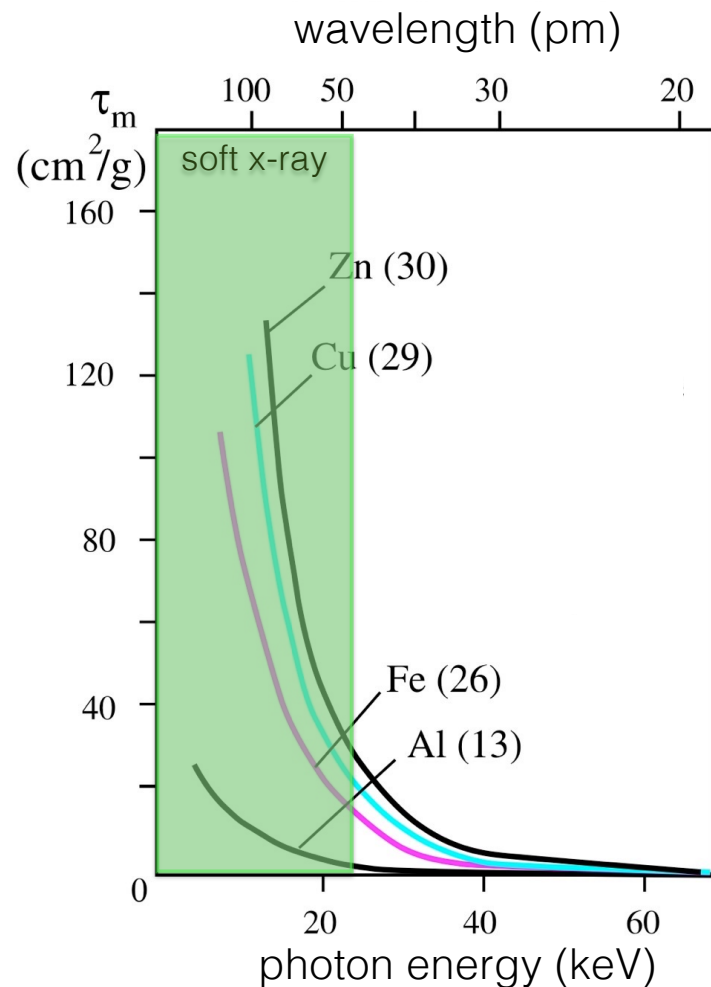
$$\mu_m = \tau_m + \sigma_m + \kappa_m$$

Mechanism	Photon energy (ϵ) dependence of the mass attenuation coefficient	Atomic number (Z) dependence of the mass attenuation coefficient	Relevant energy range in soft tissue
Photoeffect	$\sim 1 / \epsilon^3$	$\sim Z^3$	10 keV - 30 keV
Compton scatter	falls gradually with ϵ	$\sim Z/A$ (A : mass number)	30 keV - 20 MeV
Pair production	rises slowly with ϵ	$\sim Z^2$	$> 20 \text{ MeV}$

Diagnostic X-ray:

1. Contrast mechanism between soft tissue and bone: photoeffect ($\sim Z^3$)
2. Contrast mechanism within soft tissue: Compton-scatter ($\sim \rho$)

Photoeffect attenuation depends strongly on photon energy and atomic number



$$\tau_m = \text{const} \cdot \frac{Z^3}{\epsilon^3} = C \cdot \lambda^3 \cdot Z^3$$

For multi-component system:
“effective atomic number” (Z_{eff})

$$Z_{\text{eff}} = \sqrt[n]{\sum_{i=1}^n w_i Z_i^3}$$

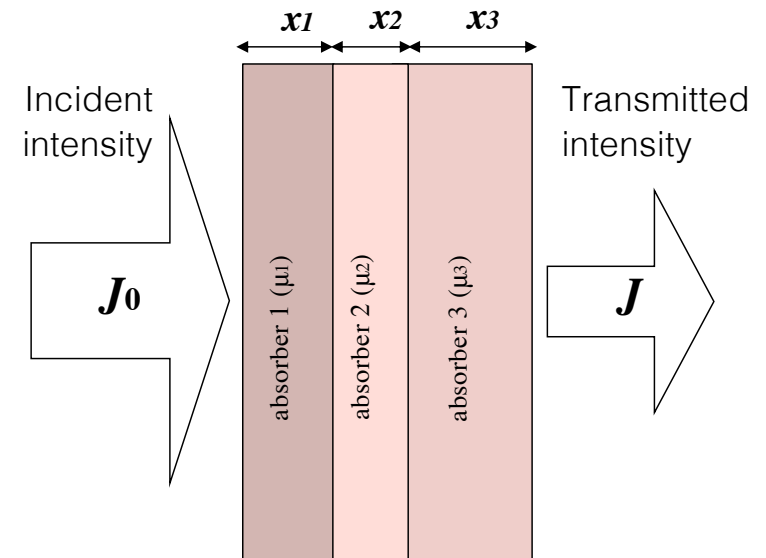
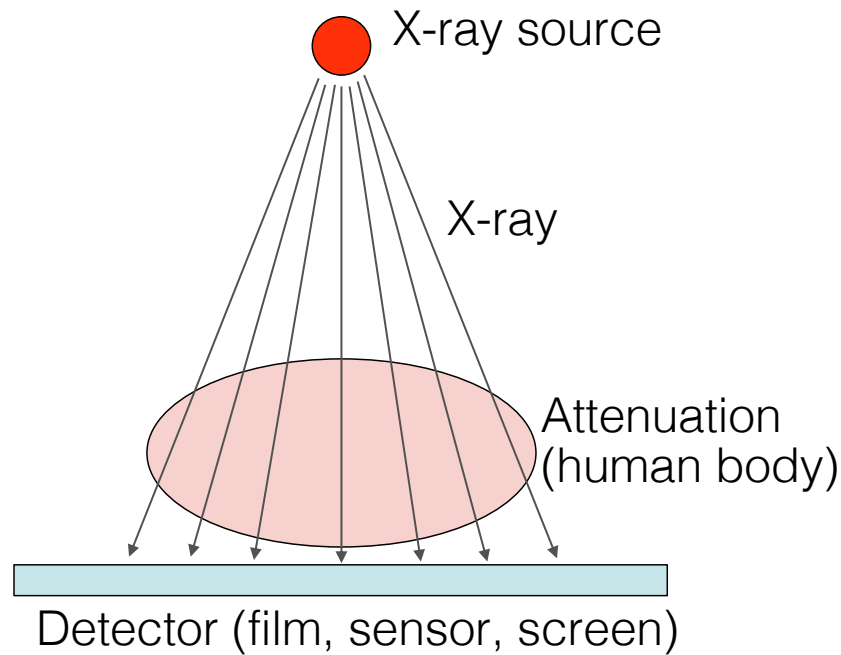
Material	Z_{eff}
Air	7.3
Water	7.7
Soft tissue	7.4
Bone	13.8

ϵ =photon energy
 Z =atomic number
 w =mole fraction
 n =number of components

At low energies ($E < 30$ keV):

$$\frac{\mu_{\text{bone}}}{\mu_{\text{soft tissue}}} \approx \frac{(\tau_{m,b} \cdot \rho_b)}{(\tau_{m,st} \cdot \rho_{st})} \approx 11$$

Application I. X-ray imaging

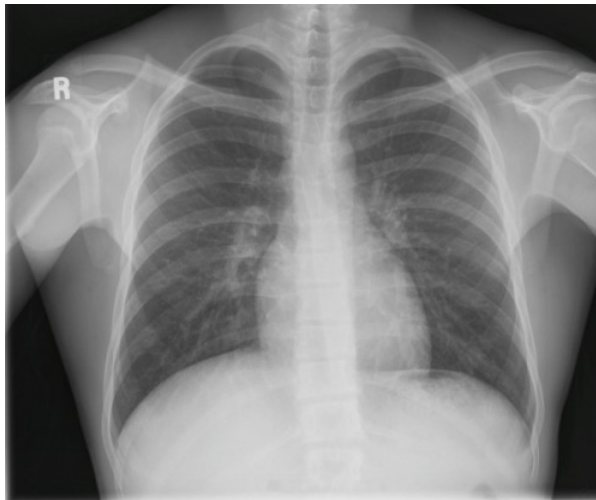


$$J = J_0 e^{-(\mu_1 x_1 + \mu_2 x_2 + \mu_3 x_3 + \dots)}$$

$$\lg \frac{J_0}{J} = (\mu_1 x_1 + \mu_2 x_2 + \mu_3 x_3 + \dots) \cdot \lg e$$

μ_n : n^{th} absorber's attenuation coefficient
 x_n : n^{th} absorber's thickness

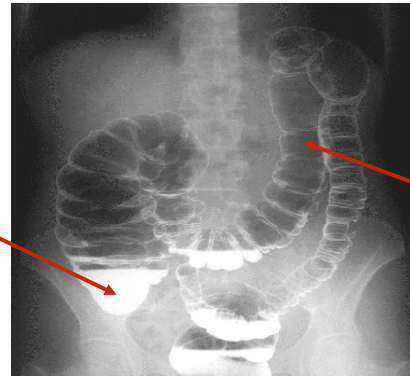
The X-ray image is a summation image ("X-ray image", "radiographic image", "roentgenogram"). Contrast arises due to spatially varying attenuation.



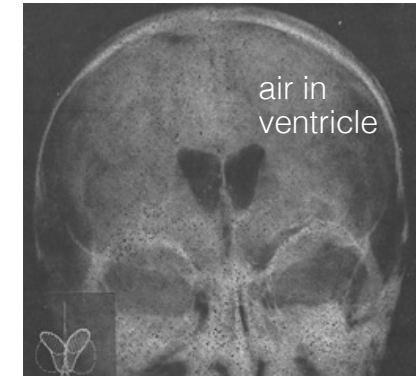
Improving X-ray imaging I.

Increasing contrast:
contrast agents

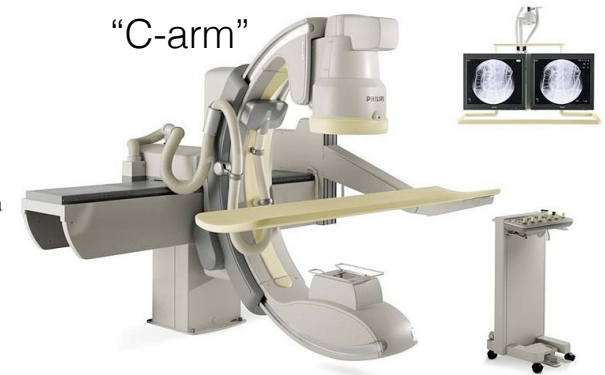
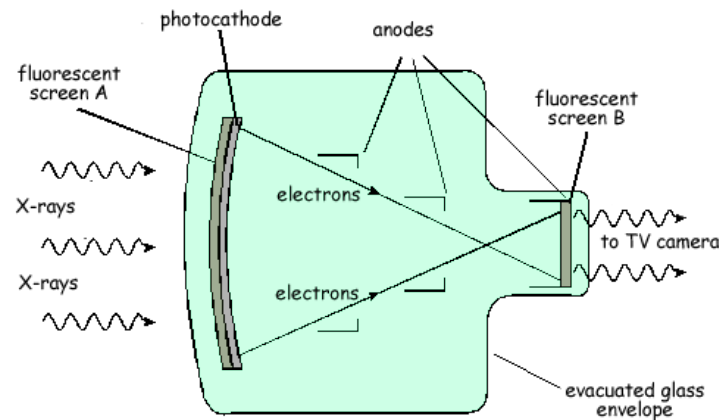
Positive contrast
(large Z ,
e.g., Ba)



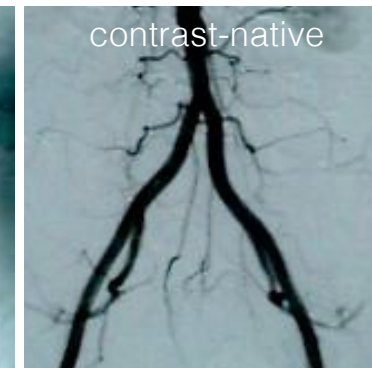
Negative contrast
(small density,
e.g., air)



Enhancing sensitivity:
intensifier



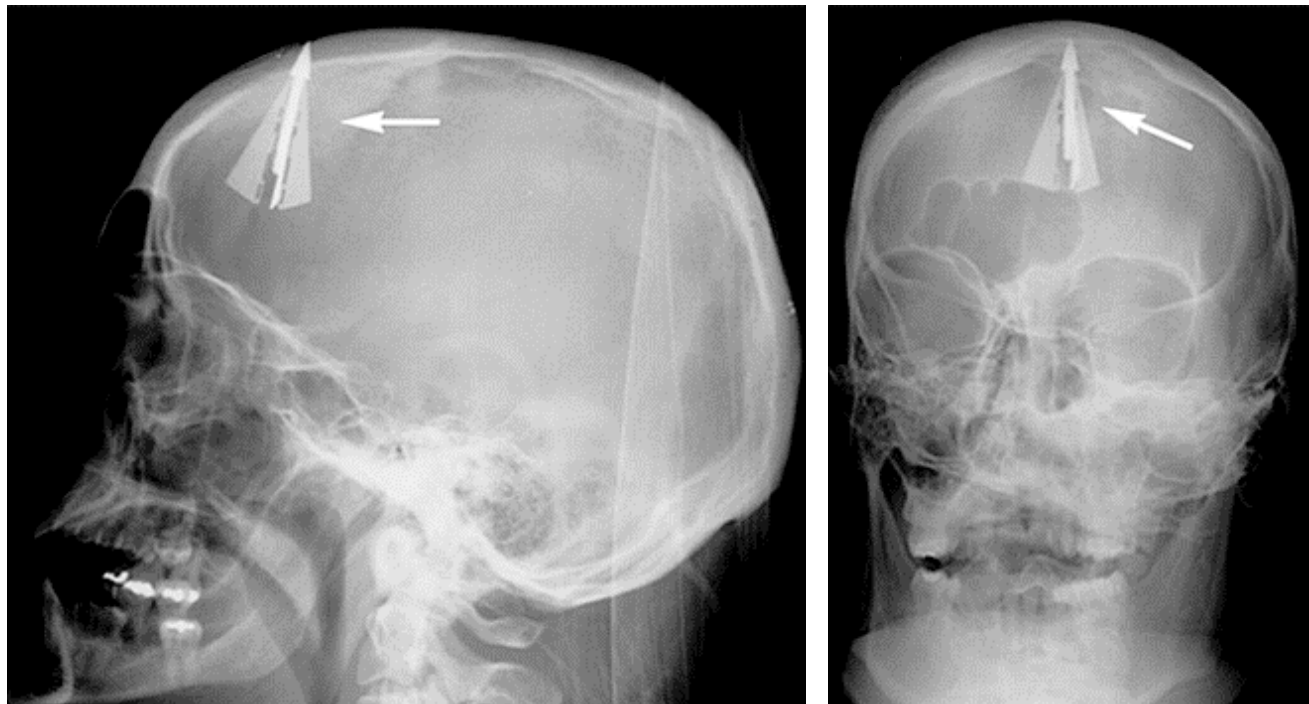
Background subtraction:
“Digital Subtraction
Angiography” (DSA)



Improving X-ray imaging II.

Spatial resolution

Bi-directional X-ray imaging



Bi-directional cranial X-ray of an individual who tried to commit suicide with a crossbow.

Improving X-ray imaging: the CAT scanner

History

- Röntgen, Hounsfield and Cormack
- 1967: first CAT scan
- 1972: prototype
- 1974: first clinical CAT image (head)
- 1976: whole body CAT scan
- 1979: Nobel-prize
- 1990: spiral CAT scanner
- 1992: multislice CAT scanner
- 2006: 64 slice (and more...)
- multiple and hybrid modes: SPECT-CT, PET-CT, Dual-source CT



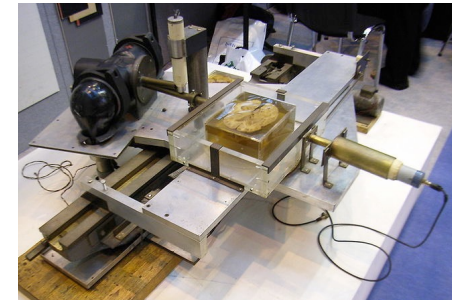
Godfrey Hounsfield



Allan Cormack



First, lab CT of a brain slice

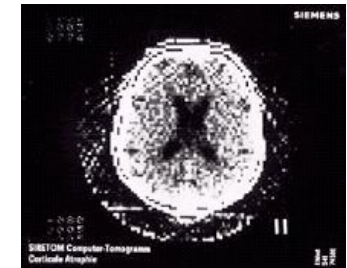


Prototype CAT scanner (EMI)

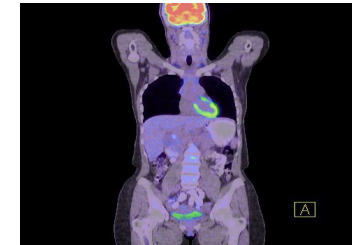
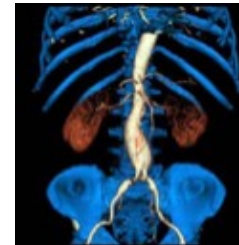


„Siretom” head scanner (1974)

128x128 pixel image (1975)



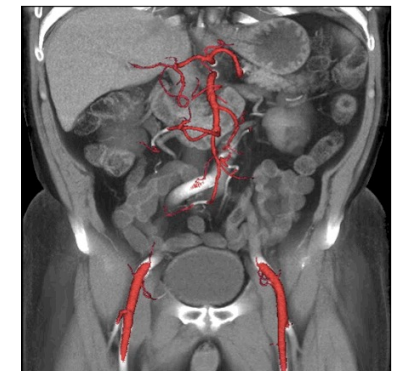
Multi-modal (combined) images



Summary

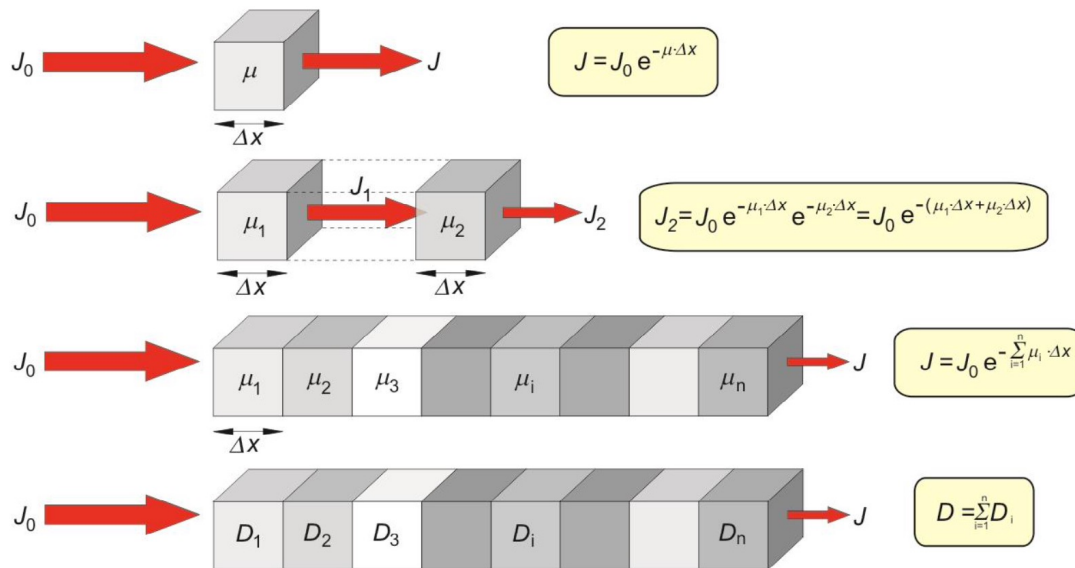
- **Tomographic** digital imaging method that uses **x-rays**: displays x-ray **absorbance** by the different points of the tomographic slice.
- **Multidetector** spiral CT (4-64 detector array): one slice 0.4-1 s; entire examination 5-15 s.
- **Ionizing** radiation. Absorbed **dose** ~50-100 times that of conventional x-ray. Significant **scattered** intensity.

Current CAT scanner



CT Foundations I: determination of μ

Objective: to determine the attenuation coefficient (μ_x) of the individual volume elements (voxels)



μ : linear attenuation coefficient
 Δx : width of the voxel

X-ray density: $D = \lg \left(\frac{J_0}{J} \right) = \lg e \cdot \mu \cdot \Delta x$

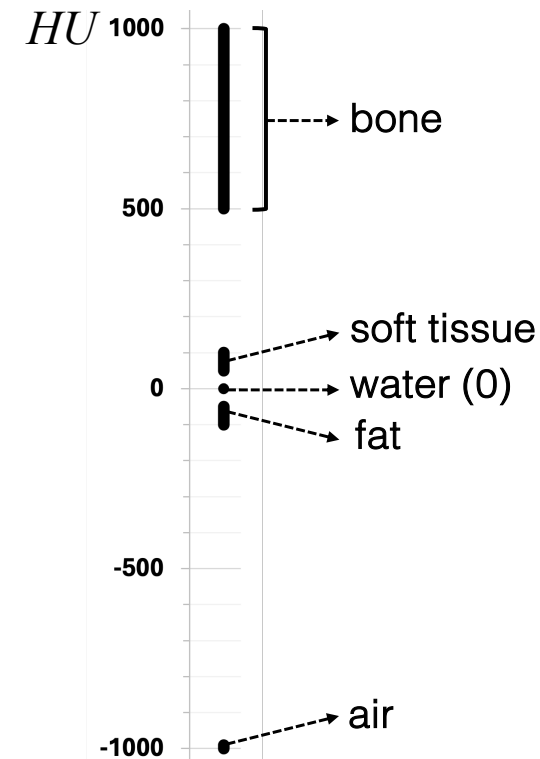
CT Image: density matrix

$$HU = 1000 \frac{\mu - \mu_w}{\mu_w}$$

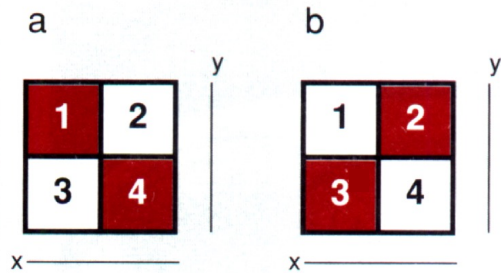
HU: Hounsfield units

μ : attenuation coefficient of voxel

μ_w : attenuation coefficient of water

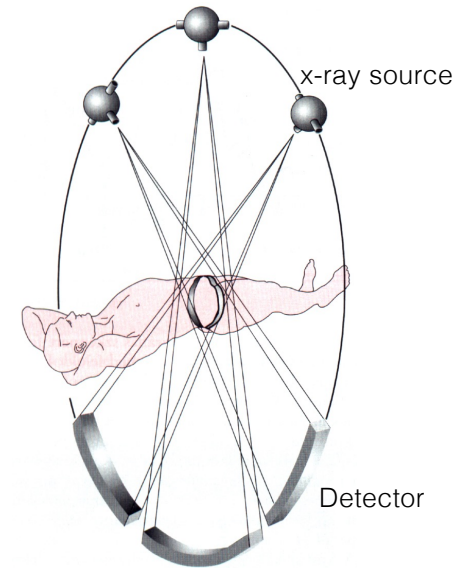


CT foundations II. scanning

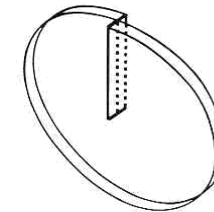
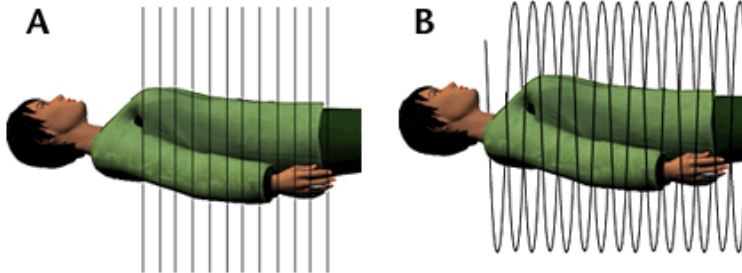
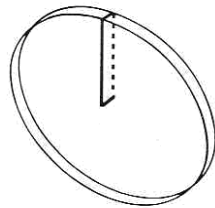


Problem: It is not possible to distinguish **a** from **b** in a bi-directional image

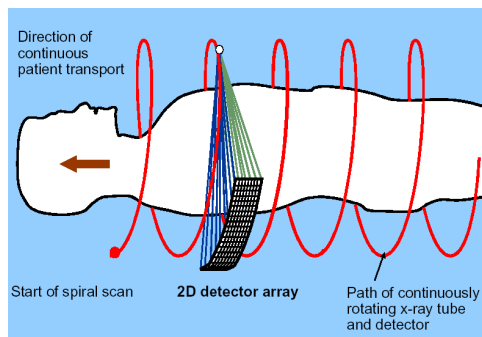
Solution: transaxial scanning along as large angular resolution as possible.



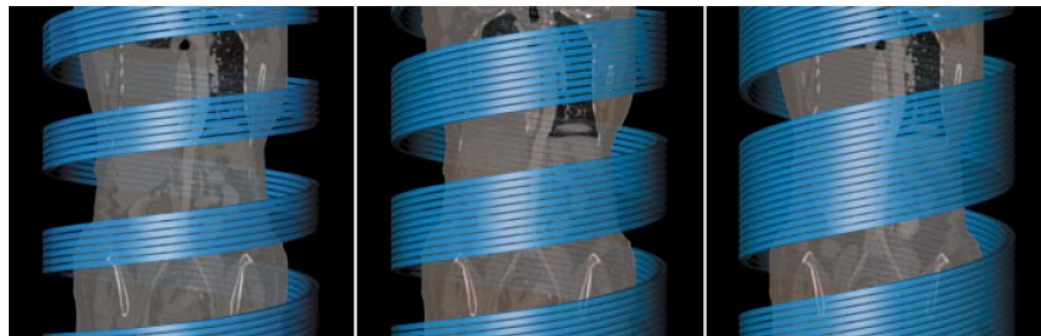
Conventional CT slice



Spiral CT slice



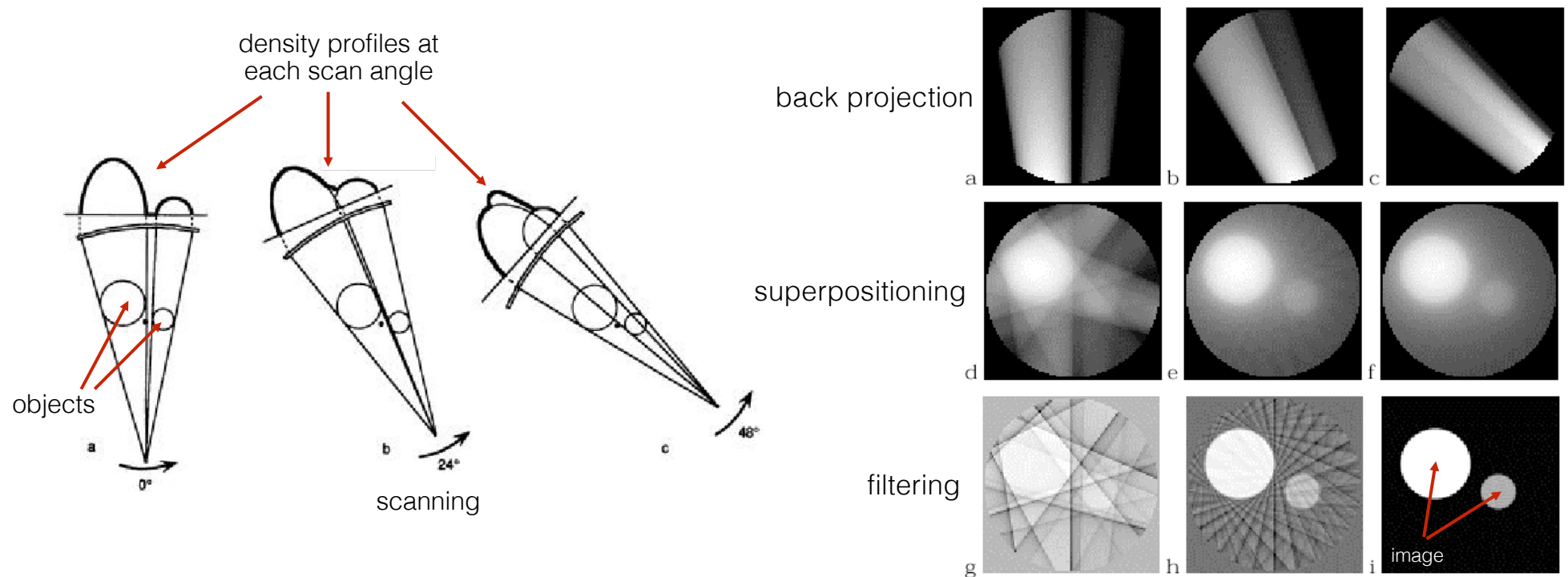
Multi-detector CT (MDCT)



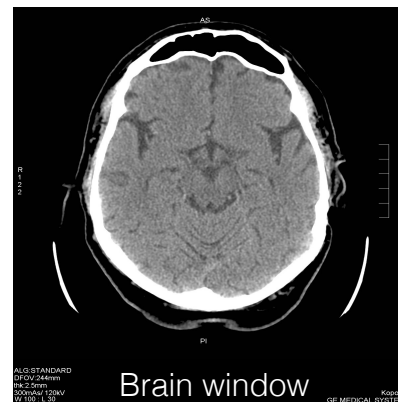
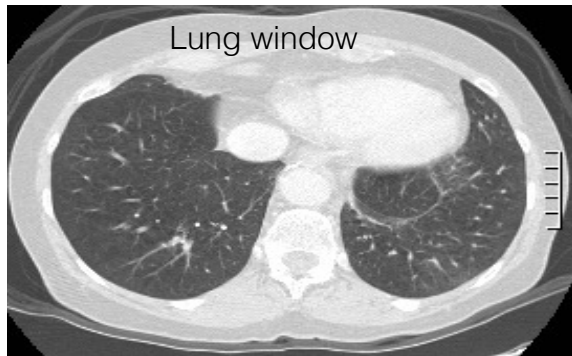
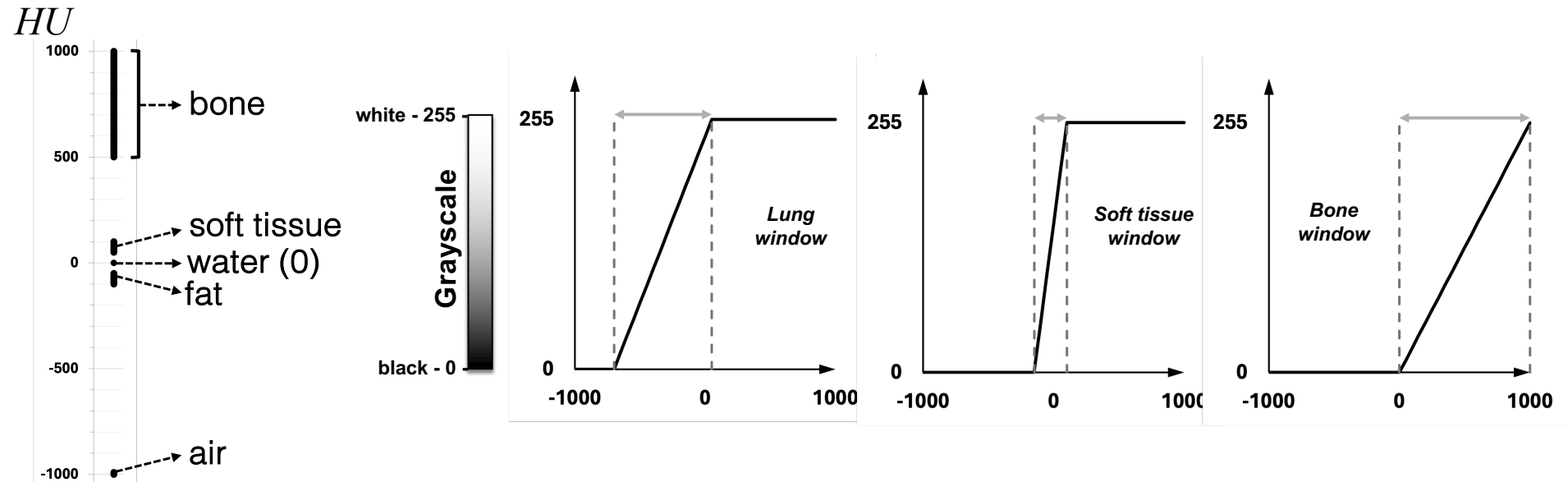
Multi-slice CT (MSCT)

CT foundations III: Image Reconstruction

1. Algebraic reconstruction techniques
2. Direct Fourier reconstruction
3. „Filtered Back Projection” (current method)

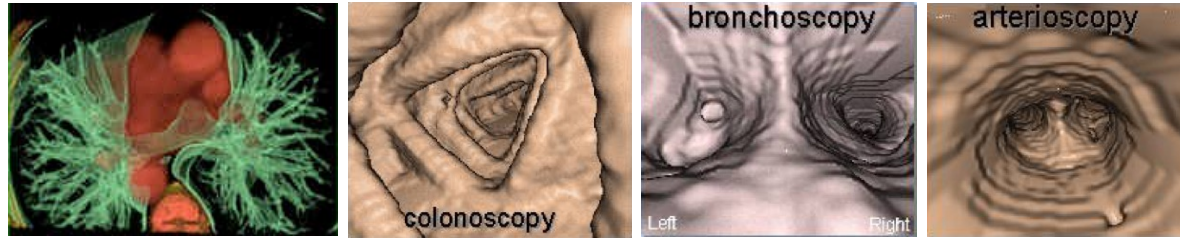


CT foundations IV: Contrast manipulation „Windowing”



Modern CAT scanning

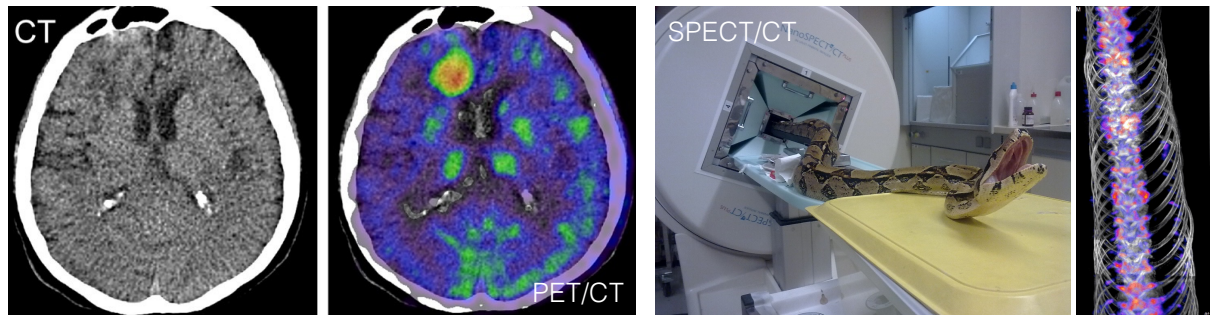
3D reconstruction,
Virtual
endoscopy



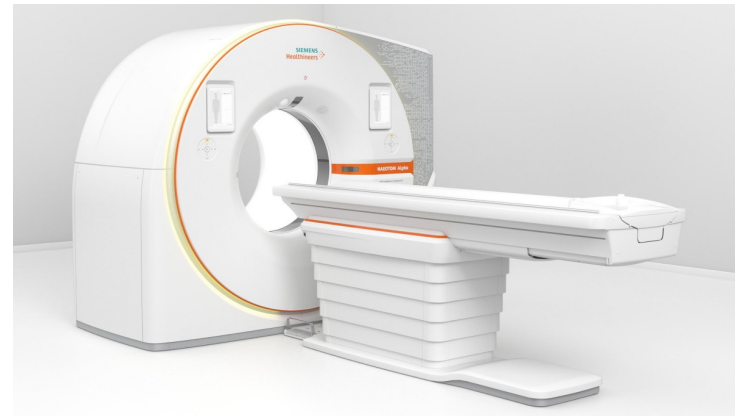
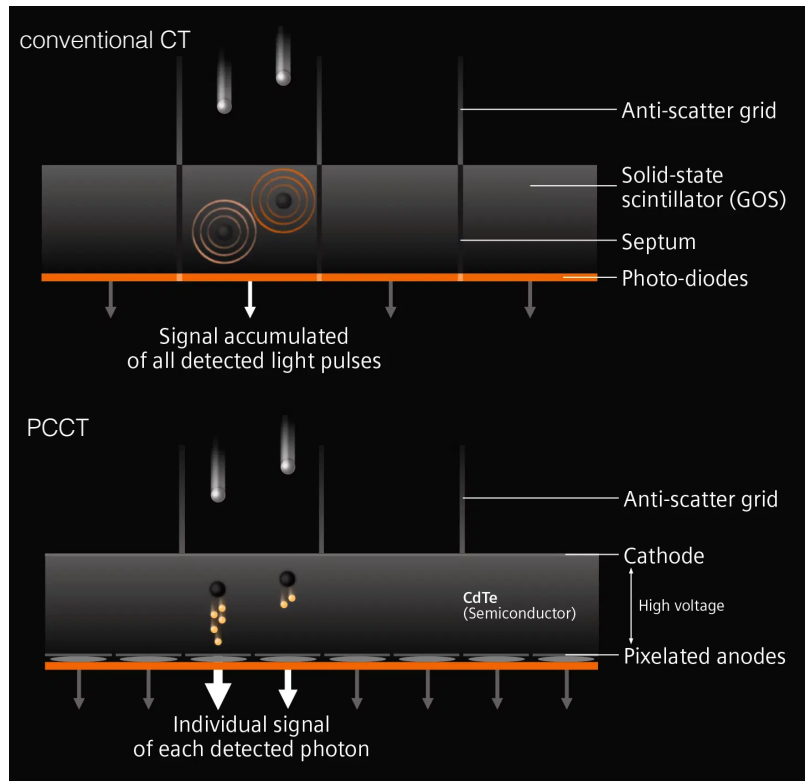
Increasing speed
and resolution



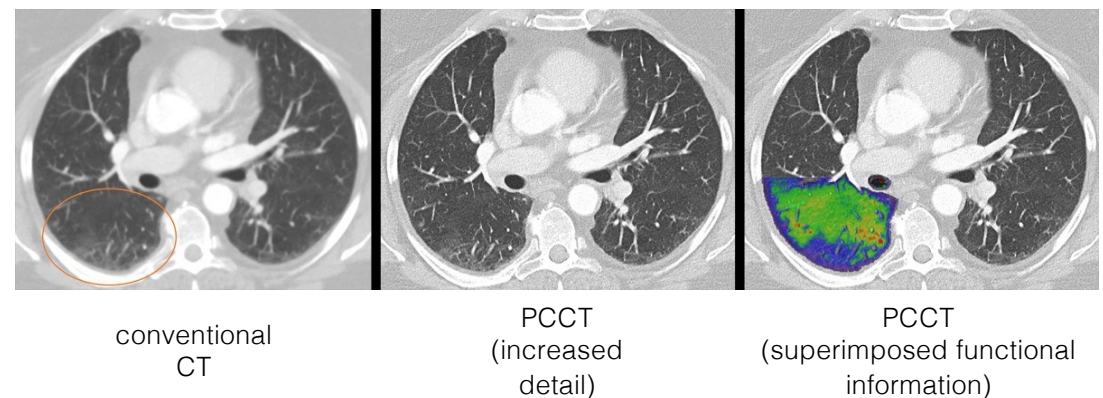
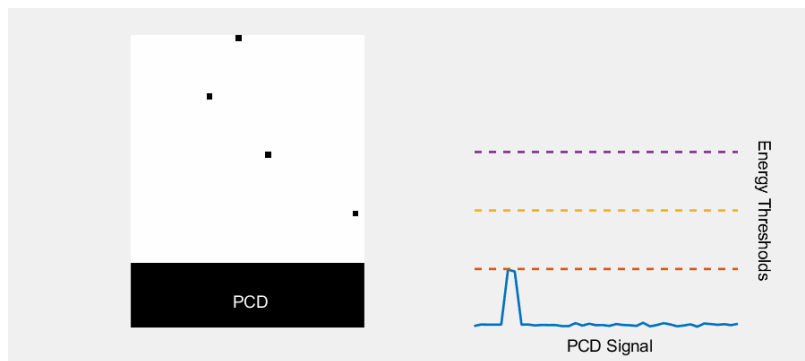
Combination with
other modalities



Photon Counting CT (PCCT)

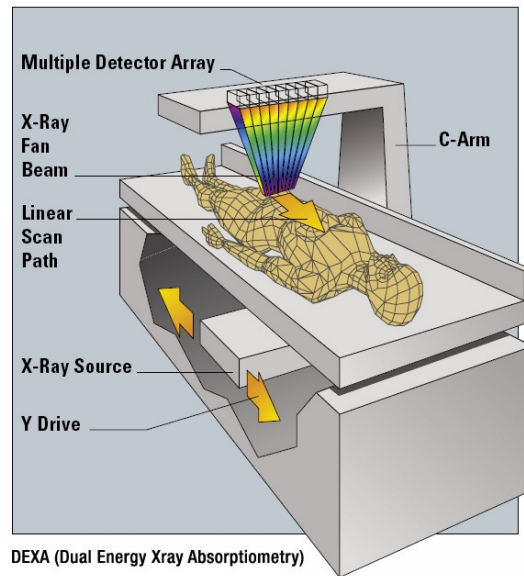


- PCD: Photon Counting Detector (cadmium telluride crystal, CdTe)
- PCD keeps track of the energy of incoming photons
- PCD provides x-ray energy spectrum
- increased sensitivity (lower x-ray dose, lower contrast-agent dose)
- functional imaging possibility



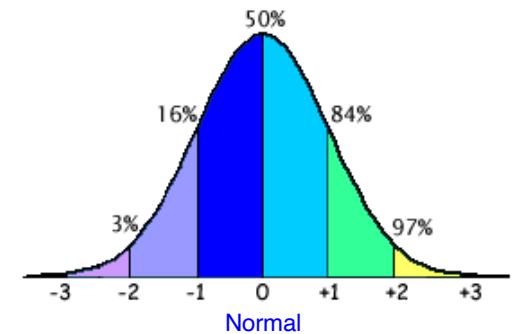
Application II. Absorptiometry

Dual-energy X-ray absorptiometry (DXA or DEXA)

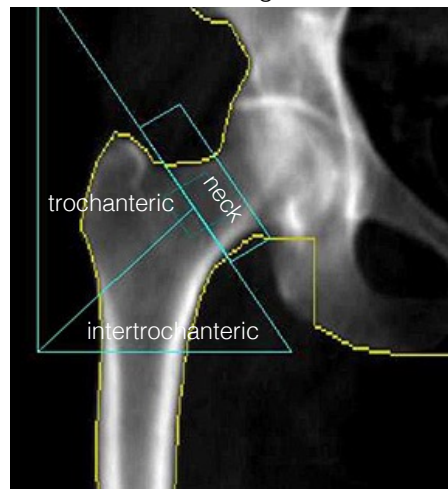


- Most important method for measuring bone density
- Characteristic X-ray is used as source
- Two different photon energies are employed (so that bone vs. soft-tissue absorption can be differentiated)
- Low dose is applied
- Whole-body scan is recorded
- Densities of distinct areas (e.g., femur, spine) are compared with reference databases
- Bone Mineral Density (BMD) calculated
- T-score is established

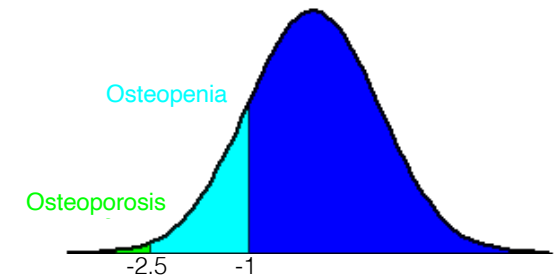
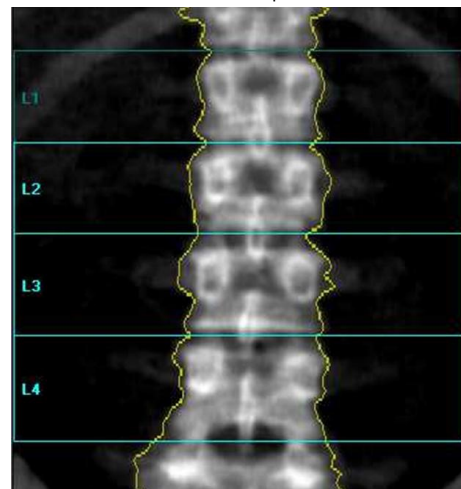
T-score:
number of standard deviations below the average for a young adult at peak bone density.



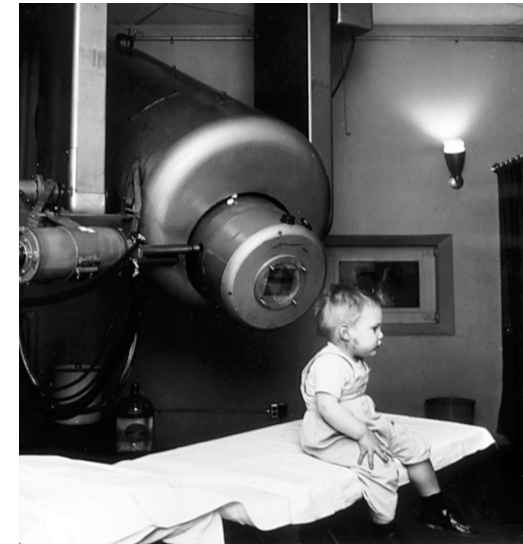
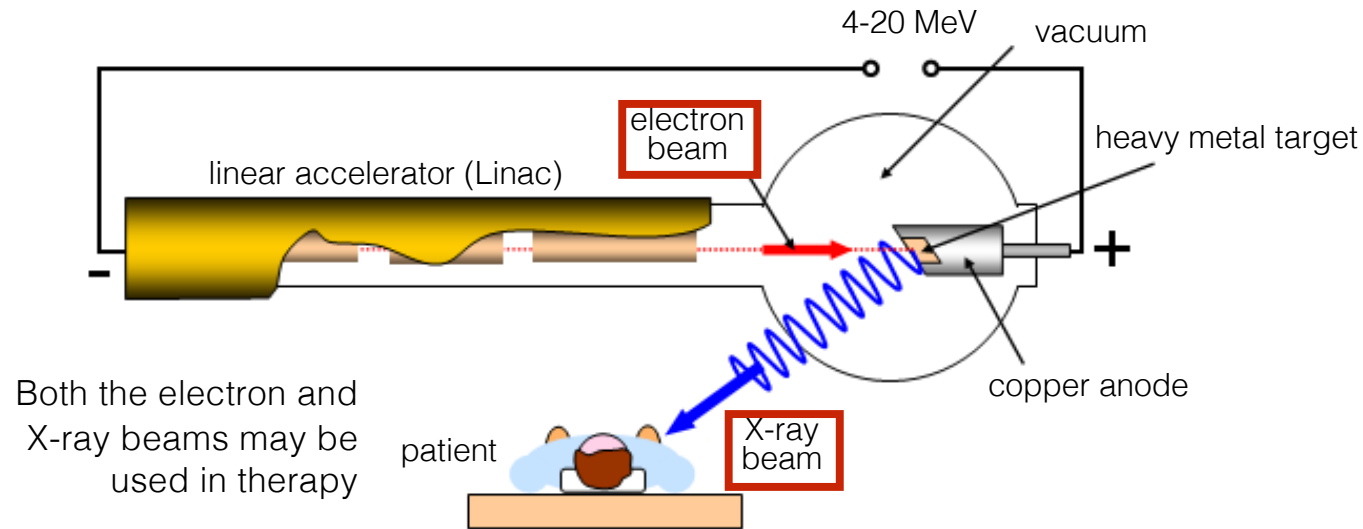
femur region



lumbar spine



Application III. Radiation therapy



First patient (Gordon Isaacs) treated with Linac radiation therapy (electron beam) for retinoblastoma (1955)



Modern hospital Linac

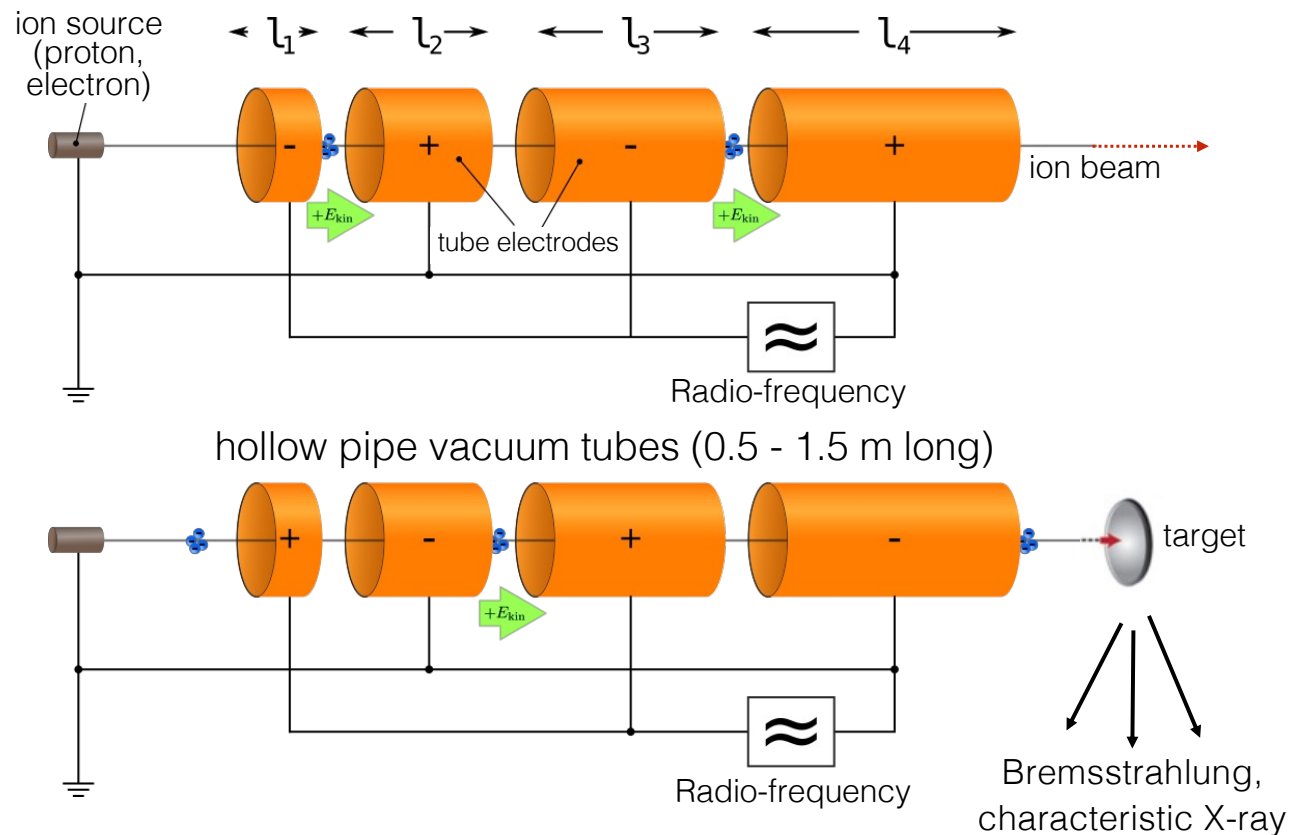
Advantages:

- Radiation may be turned on and off
- No contaminating radioactivity

Generating high-energy X-ray

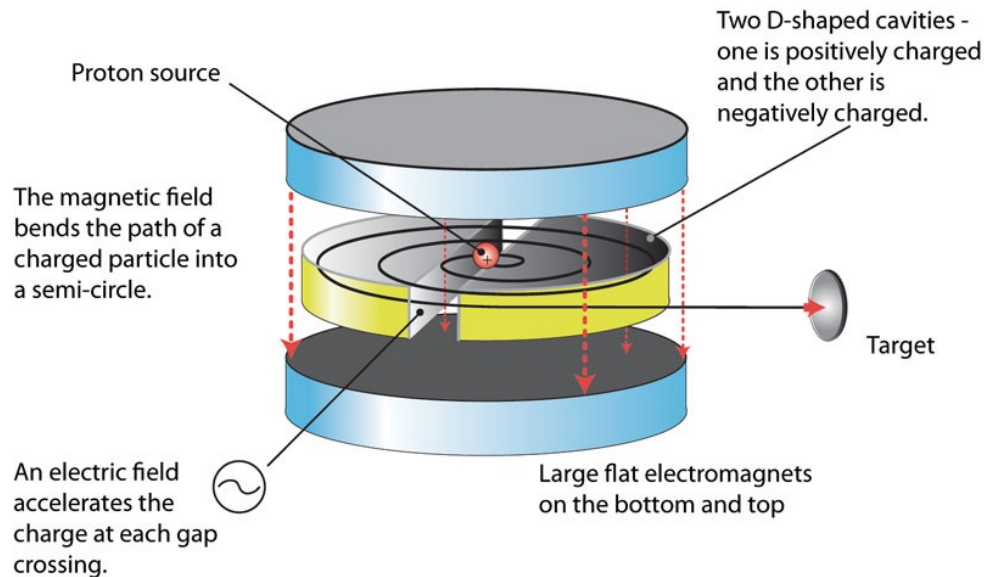
Linear accelerator (Linac)

- Charged particle (electron, proton) accelerated between electrodes (but not inside the electrode).
- Velocity of particle increases in steps.
- Electrode polarity is alternating.
- Electrodes are gradually longer (l_n increases) in order to maintain synchrony.
- Accelerated particles are directed at suitable target material (to generate X-ray).

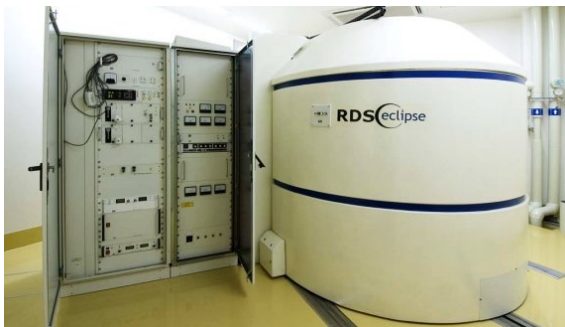


Ring-shape particle accelerators

Cyclotron

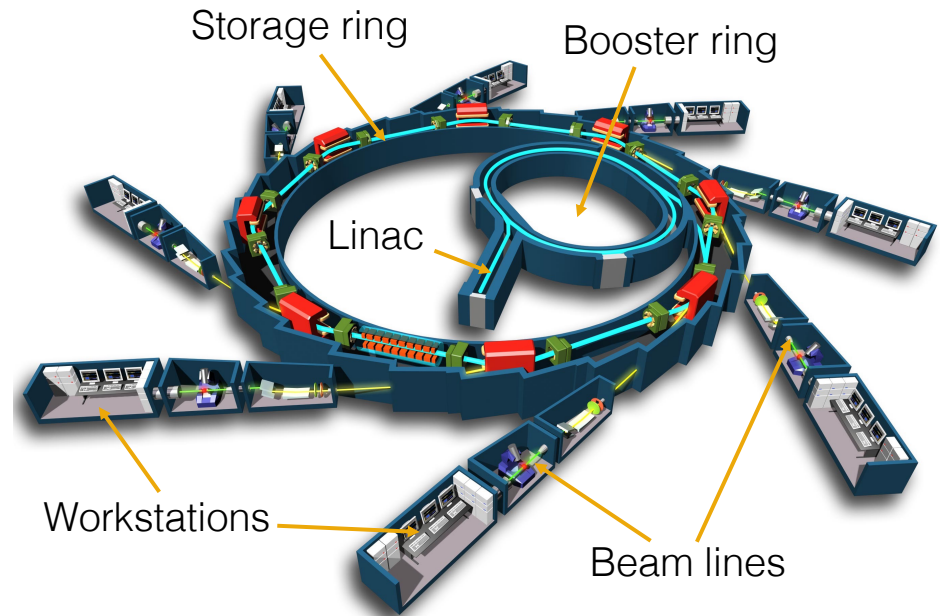


- Lorentz forces keep particles on circular path (causes limitations)
- Few tens of MeV particles are generated
- Used for generating positron-emitting isotopes (PET)
- Clinical cyclotrons in PET centers

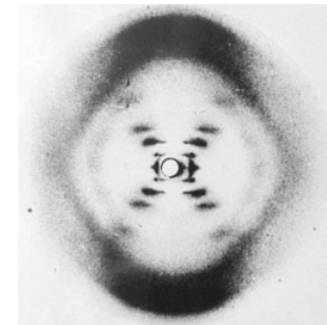
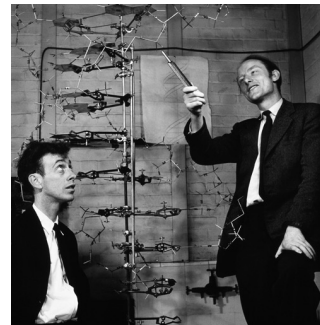


11 MeV medical cyclotron

Synchrotron



- Very high energy particles can be generated (GeV)
- Relativistic speeds can be achieved (near light speed)
- X-rays used for high-resolution structural research
- Few facilities around the world (Grenoble, Chicago, etc.)



J.D. Watson and C.F. Crick, and the first x-ray image of DNA (1953)